

# Electronic structure of relativistic Mott insulator $\text{Li}_2\text{RhO}_3$

Chao Cao,<sup>1,\*</sup> Yongkang Luo,<sup>2</sup> Zhuan Xu,<sup>2</sup> and Jianhui Dai<sup>1</sup>

<sup>1</sup>*Condensed Matter Group, Department of Physics,  
Hangzhou Normal University, Hangzhou 310036, China*

<sup>2</sup>*Department of Physics, Zhejiang University, Hangzhou 310027, China*  
(Dated: Feb. 1, 2013)

Motivated by studies of coexisting electron correlation and spin-orbit coupling effect in  $\text{Na}_2\text{IrO}_3$  and a recent experiment of its 4d analogue  $\text{Li}_2\text{RhO}_3$ , we performed first-principles calculations of the rhodium oxide compound. The experimentally observed ground state of  $\text{Li}_2\text{RhO}_3$  can be recovered only if both spin-orbit coupling and on-site Coulomb interaction are taken into consideration. Within the proper  $U$  range for 4d-orbitals ( $2 \leq U \leq 4$  eV), the ground state of  $\text{Li}_2\text{RhO}_3$  could be either zigzag-AFM or stripy-AFM, both yielding energy gap close to experimental observation. Furthermore, the total energy differences between the competing magnetic phases are  $\leq 3$  meV/Rh within  $2 \leq U \leq 4$  eV, manifesting strong magnetic frustration in the compound. Finally, the phase energy of  $\text{Li}_2\text{RhO}_3$  cannot be fitted with the two-dimensional Heisenberg-Kitaev model involving only the nearest neighbor interactions, and we propose that inter-layer interactions may be responsible for the discrepancy.

PACS numbers:

Electronic structure of transition metal oxides has been a hot topic in the condensed matter community for decades. On one hand, the 3d-transition metal oxides are considered as typical strongly correlated systems whose on-site electron-electron interactions  $U$  are large enough to forbid the hopping of electrons among lattice sites, leading to the Mott behavior. On the other hand, as the 5d-orbitals are much more extended than the 3d-orbitals, the correlation effect for 5d-orbitals are small and negligible, while its spin-orbit coupling (SOC) effect becomes prominent.

The above argument, however, is challenged by studies of 5d-metal oxide  $\text{Na}_2\text{IrO}_3$ <sup>1-10</sup>. As a 5d metal oxide,  $\text{Na}_2\text{IrO}_3$  is an ideal candidate for realizing the Heisenberg-Kitaev model

$$H_{\text{HK}} = \sum_{\langle i,j \rangle} \left[ (1 - \alpha) \hat{\mathbf{S}}_i \cdot \hat{\mathbf{S}}_j - 2\alpha S_i^\gamma S_j^\gamma \right] \quad (1)$$

where  $\gamma = x, y, z$  denotes the three different types of links in the hexagonal lattices, and  $\alpha$  indicates the interpolation between the Heisenberg term and the Kitaev term, with  $\alpha = 0$  and  $\alpha = 1$  recovering the original Heisenberg and Kitaev model, respectively. It is believed that  $\alpha$  is relatively large for 5d electron systems due to strong SOC effect. As pointed out by J. Reuther *et al.*, the ground state of the Heisenberg-Kitaev model is Néel antiferromagnetic (AFM) for  $0 \leq \alpha < 0.4$ , and stripy AFM for  $0.4 \leq \alpha < 0.8$ . When the Kitaev term becomes dominantly large where  $0.8 \leq \alpha < 1$ , the system will enter a spin-liquid phase<sup>11</sup>. However, it was later discovered in both first-principles calculations and experiments that the ground state for  $\text{Na}_2\text{IrO}_3$  is indeed the zigzag AFM phase, and the material is a relativistic Mott insulator<sup>2,4</sup>. To resolve the apparent discrepancy, it was proposed that a next-nearest-neighbor Heisenberg coupling term should be added into the original Heisenberg-Kitaev model<sup>7</sup>. On the contrary, I. I. Mazin *et al.* questioned the application

of localized spin models in the system, and proposed a quasi-molecular-orbital approach<sup>3</sup>.

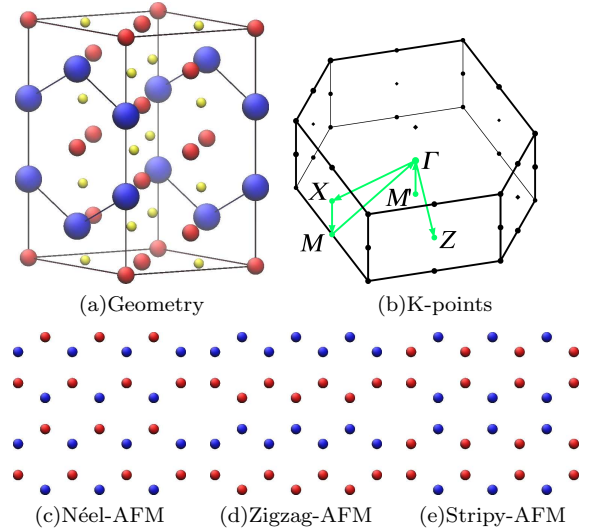


FIG. 1: (a) Crystal structure of  $\text{Li}_2\text{RhO}_3$ . The blue large atoms are Rh; red smaller atoms are Li; and yellow smallest atoms are O. The hexagonal lattice of Rh is also shown. (b) The first irreducible Brillouin zone and the high symmetry points appeared in this paper. (c-e) The Néel-AFM, zigzag-AFM, and stripy-AFM configurations for hexagonal lattices. The red and blue spheres indicates spin up and down Rh atoms, respectively.

Recently, 4d-transition metal oxide  $\text{Li}_2\text{RhO}_3$  was reported to be in close proximity to spin glassy phase<sup>12</sup>. As the 4d systems usually have moderate Coulomb interaction and SOC in between 3d and 5d systems, this 4d compound should be very interesting not only because of its structural analogue to  $\text{Na}_2\text{IrO}_3$ , but also due to the more delicate interplay between the Coulomb correlation and SOC. It was determined experimentally that no long-

$U(\text{eV})$	NM	Néel	Stripy	Zigzag	FM	NM <sup>soC</sup>	Néel <sup>soC</sup>	Stripy <sup>soC</sup>	Zigzag <sup>soC</sup>	FM <sup>soC</sup>
0.0	-138.1672	-138.1672	-138.2221	-138.1994	<i>-138.3524</i>	-138.8865	-138.8867	-138.9260	-138.9170	<b>-139.0421</b>
1.0	-134.5490	-134.6043	-134.6979	-134.6441	<i>-134.8125</i>	-135.2827	-135.4302	-135.4407	-135.4610	<b>-135.5143</b>
2.0	-131.0182	-131.3321	-131.3295	-131.2195	<i>-131.3751</i>	-131.7448	-132.2128	-132.2182	<b>-132.2294</b>	-132.2102
3.0	-127.5755	-128.2610	-128.2703	-128.1069	<i>-128.2904</i>	-128.2831	-129.1358	-129.1415	<b>-129.1459</b>	-129.1332
4.0	-124.1958	-125.2890	-125.3068	-125.1276	<i>-125.3149</i>	-124.8964	-126.1658	<b>-126.1723</b>	-126.1492	-126.1652

TABLE I: Total energies (per unit cell, four Ru atoms) of different  $\text{Li}_2\text{RhO}_3$  magnetic phases. Columns 2-6 are for the calculations without SOC; while columns 7-11 are for the calculations with SOC. The lowest phase energy at different  $U$  with and without SOC are indicated with italic and bold fonts, respectively.

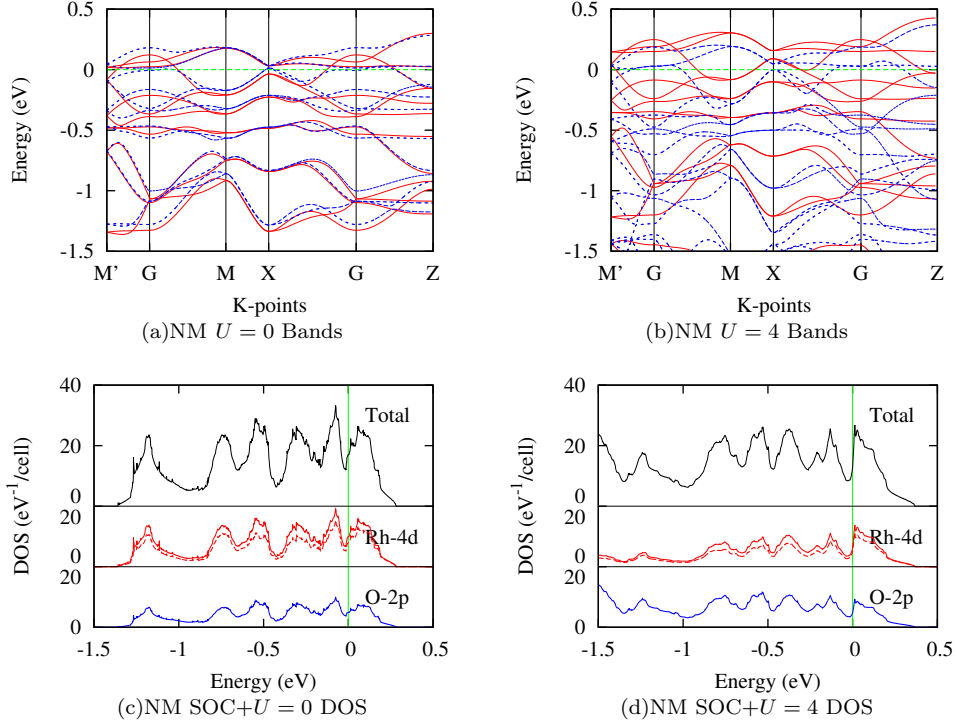


FIG. 2: (a-b): Band structure of NM phase without (red solid lines) and with (blue dashed lines) SOC. (c-d): Total and partial DOS of NM phase with SOC. (a) and (c):  $U=0$  eV. (b) and (d):  $U=4$  eV.

range magnetic order was observed in  $\text{Li}_2\text{RhO}_3$  down to 0.5 K, and spin-freezing temperature was measured to be around 6 K. Fitting of the resistivity data suggested that the compound was a semiconductor with a narrow band gap of  $\sim 78$  meV. It is worthy noting that anti-site disorder effect between  $\text{Li}^+$  and  $\text{Rh}^{4+}$  ions is inevitable in the experiment, therefore it is yet to be determined whether the spin-glassy feature is intrinsic or due to the anti-site defects. The experiment therefore raises several interesting questions: 1. Is the narrow band gap due to electron correlation or spin-orbit coupling effect? 2. How close is the defect-free  $\text{Li}_2\text{RhO}_3$  to the spin-glassy phase? 3. How relevant is the system to the Heisenberg-Kitaev model?

In this article, we present our latest first principles study of the 4d-transition metal oxide  $\text{Li}_2\text{RhO}_3$ . We calculated and compared the total energy of its magnetic

ordered phases with and without SOC effect as well as for different on-site interaction  $U$ . We analyzed its band structure and density of states (DOS) at different  $U$ 's with and without SOC. We conclude that, both the SOC and on-site interaction  $U$  are important in the compound, and the energy gap is indeed a correlation effect. Moreover, the magnetism in  $\text{Li}_2\text{RhO}_3$  is extremely frustrated, and thus the system may be very close to spin disordered phase. Finally, attempts to fit the total energy data with Heisenberg-Kitaev model failed, suggesting that interactions beyond original Heisenberg-Kitaev model may be required to understand the magnetism of the system.

To study the magnetic and electronic properties of  $\text{Li}_2\text{RhO}_3$ , we performed density functional based first principles calculations. In particular, we used the plane-wave basis and projected augmented wave method<sup>13</sup> as implemented in the Vienna Abinitio Simulation Package

(VASP)<sup>14,15</sup>. The Perdew, Burke, and Ernzerhoff flavor (PBE)<sup>16</sup> of generalized gradient approximation (GGA) were chosen to be the exchange-correlation functional. To ensure the convergence of total energy to 1 meV/cell, a high energy cut-off of 540 eV to the plane wave basis was chosen; while a dense  $8 \times 5 \times 8$   $\Gamma$ -centered K-grid was used to perform the Brillouin zone integration. The lattice constants and internal atomic positions were optimized so that the forces on individual atoms are smaller than 1 meV/Å and internal stress less than 0.04 kbar. The density of states (DOS) were calculated using a  $16 \times 10 \times 16$   $\Gamma$ -centered K-grid and tetrahedron method.

Solution of the Heisenberg-Kitaev model suggested three possible AFM ground states for hexagonal lattices<sup>10,17,18</sup>, which are also used to study the magnetic phases of  $\text{Na}_2\text{IrO}_3$ <sup>7,8</sup> (FIG. 1(c)-1(e)). In our current study, we performed calculations for all three AFM states, as well as ferromagnetic (FM) state and non-magnetic (NM) state. The total energies of different magnetic phases are listed in TABLE I.

Our calculations demonstrate that the SOC effect do play an essential role in determining the ground state magnetism. The FM phase is always the ground state if SOC is not included in the calculation, although the magnetic frustration is greatly enhanced with respect to increased  $U$ , as indicated by the reduction of the total energy difference between the FM phase and the second lowest phase (from  $\sim 32$  meV/Rh at  $U = 0$  eV to  $\sim 2$  meV/Rh at  $U = 4$  eV). With the SOC being correctly accounted for, the ground state of  $\text{Li}_2\text{RhO}_3$  starts from the FM phase at  $U = 0$  eV to the zigzag AFM phase at  $U = 2$  eV, and eventually becomes stripy AFM phase at  $U = 4$  eV. It is worthy noting that once the AFM ground state is established, the total energy difference between the ground state and second lowest phase does not exceed 12 meV/cell (or 3 meV/Rh) (11 meV/cell at  $U = 2$  eV, 4 meV/cell at  $U = 3$  eV, and 7 meV/cell at  $U = 4$  eV). By comparison, the total energy difference between the NM phase and the highest magnetic phase is at least one order of magnitude larger (465 meV/cell at  $U = 2$  eV, 850 meV/cell at  $U = 3$  eV, 1253 meV/cell at  $U = 4$  eV). Such small energy difference between magnetic phases compared with the large magnetic energy manifests strong frustrations of magnetic interactions, and that the system may be very close to spin-glass or spin-liquid phases.

We now turn to the electronic structure of  $\text{Li}_2\text{RhO}_3$ . Firstly, we compare the band structure of NM  $\text{Li}_2\text{RhO}_3$  calculated without (Fig. 2(a)) and with (Fig. 2(b)) SOC. Moderate band splitting due to SOC are normally expected for 4d-transition metals. However, for the current system, the major SOC effect is the band reordering around  $\Gamma$  from  $E_F - 0.5$  eV to  $E_F + 0.2$  eV and from  $E_F - 1.5$  eV to  $E_F - 0.8$  eV. Nevertheless, a  $\sim 86$  meV band splitting due to SOC can still be identified around  $\Gamma$  at  $\sim E_F - 1.0$  eV, which signals the strength of the SOC. Fig. 2(c) and 2(d) show the total density of states (DOS) as well as the projected density of states (PDOS) of NM

$\text{Li}_2\text{RhO}_3$  without and with SOC, respectively. Evidently, the electron states near Fermi level are contributed by the Rh-4d orbitals and O-2p orbitals, which hybridize significantly over a wide energy range. The  $t_{2g}$  orbitals of rhodium due to the octahedral crystal field dominate the 4d contributions. At the NM phase, the system remains metallic even LDA+ $U$ +SOC is employed with  $U$  up to 4 eV.

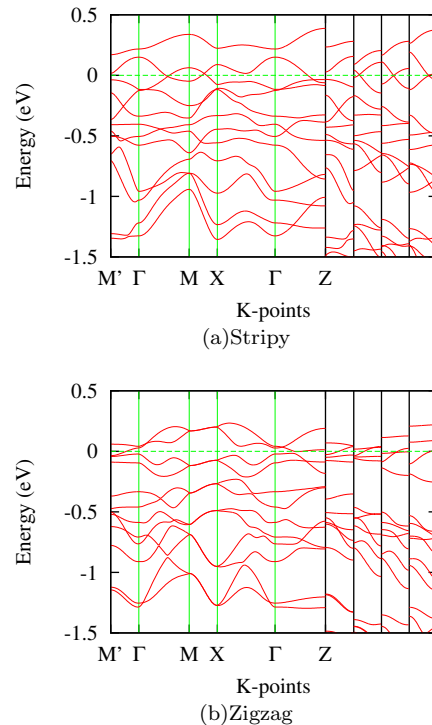


FIG. 3: Band structure of (a) zigzag and (b) stripy phases without considering SOC effect at different  $U$  level. The larger panel in each subfigure shows the band structure at  $U = 0$  eV; while the rest four smaller panels from left to right correspond to  $U = 1, 2, 3, 4$  eV, respectively. To save space, only the band structure from  $M'$  to  $\Gamma$  is shown for  $U \neq 0$  cases.

Secondly, we examine the electronic structure of  $\text{Li}_2\text{RhO}_3$  at the zigzag- and stripy-AFM phases.<sup>19</sup> Although the AFM phases cannot be stabilized unless SOC is turned on, it is instructive to compare the electronic structure at different on-site  $U$  without SOC first (FIG. 3). The large on-site energy pushes away the bands near the Fermi level, causing significant reduction of electron states at  $E_F$ . However, the electron-electron correlation alone cannot drive the system insulating, since the band gap is not opened even with  $U$  as high as 4 eV. With SOC, the system is also metallic at  $U = 0$  eV, although significant band reordering effect similar to the one observed in the NM case is also present in both AFM cases (FIG. 4(a) and 4(b)). However, a  $\sim 10$  meV energy gap immediately opens even with a small on-site energy  $U = 1$  eV in the zigzag-AFM phase. The gap grows to  $\sim 75$  meV and  $\sim 130$  meV, if the on-site energy  $U$  is increased to 2 eV

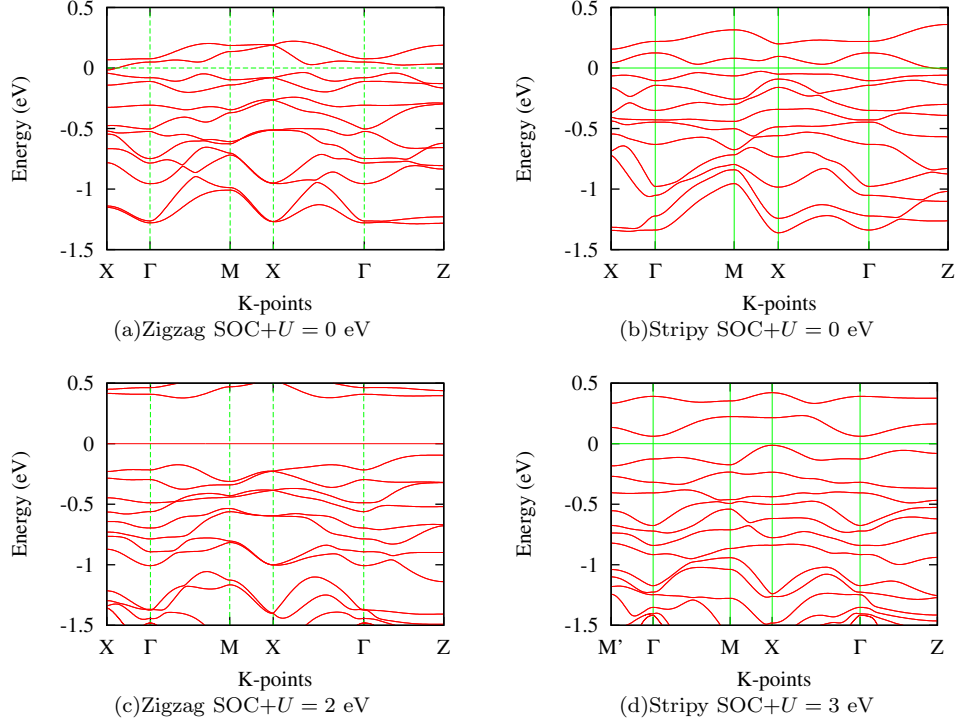


FIG. 4: Band structure of (a)(c) zigzag and (b)(d) stripy phases with SOC effect at different  $U$  level.

and 3 eV, respectively. Noticing that the experimentally observed  $E_g$  is 78 meV, which is very close to the calculated value for zigzag-AFM phase at  $U = 2$  eV (FIG. 4(c)). The magnetic moment is found to be  $\sim 0.4 \mu_B/\text{Rh}$ , twice the value for the one in the zigzag-AFM phase of  $\text{Na}_2\text{IrO}_3^3$ . For the stripy-AFM phase, a relatively larger  $U = 2$  eV is required to open an diminishing energy gap of 3 meV. The gap expands to  $\sim 62$  meV and 117 meV for  $U = 3$  eV and  $U = 4$  eV, respectively. The magnetic moment is  $\sim 0.2 \mu_B/\text{Rh}$  in this phase, similar to the value for the one in the stripy-AFM phase of  $\text{Na}_2\text{IrO}_3^3$ . As the zigzag-AFM and stripy-AFM phases are energetically very close around  $U = 3$  eV ( $\sim 1$  meV/Rh), one cannot deduce the ground state magnetic ordering from the comparison between the calculation and experiment. Once again, the two phases severely competes with each other, and fluctuations (quantum or thermal) can easily drive the system into disordered spin states. Nevertheless, in each case the system is non-metallic with a small gap of 60~120 meV.

We want to make some further remarks regarding the obtained results. The calculated band structure in all magnetic phases appear to be quite three-dimensional. In fact, the inter-layer Rh-Rh distances are  $\sim 5.1 \text{ \AA}$  still comparable with the intra-layer Rh-Rh distance of 3.03  $\text{\AA}$ . Therefore, it is questionable whether two-dimensional Heisenberg-Kitaev model is applicable to such system. Indeed, when we attempted to fit the phase energy data to the classical results of the Heisenberg-Kitaev model<sup>17</sup>, the fitting failed for all  $U$ , as the fitted  $J$  and  $\alpha$  result

in a wrong phase energy order. Therefore, it is possible that interactions beyond the original Heisenberg-Kitaev model is required to describe the system. Considering the three-dimensional feature of its electronic structure, we propose it is likely to be the inter-layer coupling  $J_c$ .

In conclusion, we have performed first-principles study of  $\text{Li}_2\text{RhO}_3$ , comparing the electronic structure and energetics of different magnetic phases with or without SOC effect at  $U$  ranging from 0 to 4 eV. Both SOC and on-site electron correlation are crucial in determining the electronic structure of the compound. Within the proper  $U$  range, the compound is semiconducting with a small gap of  $\sim 60$  to  $\sim 120$  meV; and the energy difference between the competing magnetic phases are extremely small, suggesting highly frustrated magnetism in the system and that the system may be in close proximity to disordered spin state. Since the phase energies do not fit well with classical Heisenberg-Kitaev model results and its electronic structure is highly three-dimensional, we propose that inter-layer coupling  $J_c$  may be required to explain the behavior of the system.

### Acknowledgments

This work has been supported by the NSFC (No. 11274006, No. 11274084) and the NSF of Zhejiang Province (No. LR12A04003, Z6110033). All calculations were performed at the High Performance Computing Center of Hangzhou Normal University College of

Science.

- 
- \* E-mail address: ccao@hznz.edu.cn
- <sup>1</sup> H. Gretarsson, J. P. Clancy, X. Liu, J. P. Hill, E. Bozin, Y. Singh, S. Manni, P. Gegenwart, J. Kim, A. H. Said, et al., Phys. Rev. Lett. **110**, 076402 (2013), URL <http://link.aps.org/doi/10.1103/PhysRevLett.110.076402>.
  - <sup>2</sup> F. Ye, S. Chi, H. Cao, B. C. Chakoumakos, J. A. Fernandez-Baca, R. Custelcean, T. F. Qi, O. B. Korneta, and G. Cao, Phys. Rev. B **85**, 180403 (2012), URL <http://link.aps.org/doi/10.1103/PhysRevB.85.180403>.
  - <sup>3</sup> I. I. Mazin, H. O. Jeschke, K. Foyevtsova, R. Valentí, and D. I. Khomskii, Phys. Rev. Lett. **109**, 197201 (2012), URL <http://link.aps.org/doi/10.1103/PhysRevLett.109.197201>.
  - <sup>4</sup> R. Comin, G. Levy, B. Ludbrook, Z.-H. Zhu, C. N. Veenstra, J. A. Rosen, Y. Singh, P. Gegenwart, D. Stricker, J. N. Hancock, et al., Phys. Rev. Lett. **109**, 266406 (2012), URL <http://link.aps.org/doi/10.1103/PhysRevLett.109.266406>.
  - <sup>5</sup> H.-C. Jiang, Z.-C. Gu, X.-L. Qi, and S. Trebst, Phys. Rev. B **83**, 245104 (2011), URL <http://link.aps.org/doi/10.1103/PhysRevB.83.245104>.
  - <sup>6</sup> A. Shitade, H. Katsura, J. Kuneš, X.-L. Qi, S.-C. Zhang, and N. Nagaosa, Phys. Rev. Lett. **102**, 256403 (2009), URL <http://link.aps.org/doi/10.1103/PhysRevLett.102.256403>.
  - <sup>7</sup> Y. Singh, S. Manni, J. Reuther, T. Berlijn, R. Thomale, W. Ku, S. Trebst, and P. Gegenwart, Phys. Rev. Lett. **108**, 127203 (2012), URL <http://link.aps.org/doi/10.1103/PhysRevLett.108.127203>.
  - <sup>8</sup> S. K. Choi, R. Coldea, A. N. Kolmogorov, T. Lancaster, I. I. Mazin, S. J. Blundell, P. G. Radaelli, Y. Singh, P. Gegenwart, K. R. Choi, et al., Phys. Rev. Lett. **108**, 127204 (2012), URL <http://link.aps.org/doi/10.1103/PhysRevLett.108.127204>.
  - <sup>9</sup> C. H. Kim, H. S. Kim, H. Jeong, H. Jin, and J. Yu, Phys. Rev. Lett. **108**, 106401 (2012), URL <http://link.aps.org/doi/10.1103/PhysRevLett.108.106401>.
  - <sup>10</sup> J. c. v. Chaloupka, G. Jackeli, and G. Khaliullin, Phys. Rev. Lett. **110**, 097204 (2013), URL <http://link.aps.org/doi/10.1103/PhysRevLett.110.097204>.
  - <sup>11</sup> J. Reuther, R. Thomale, and S. Trebst, Phys. Rev. B **84**, 100406 (2011), URL <http://link.aps.org/doi/10.1103/PhysRevB.84.100406>.
  - <sup>12</sup> Y. Luo, C. Cao, B. Si, Y. Li, J. Bao, H. Guo, X. Yang, C. Shen, C. Feng, J. Dai, et al., ArXiv e-prints (2013), 1303.1235.
  - <sup>13</sup> P. E. Blöchl, Phys. Rev. B **50**, 17953 (1994), URL <http://link.aps.org/doi/10.1103/PhysRevB.50.17953>.
  - <sup>14</sup> G. Kresse and J. Hafner, Phys. Rev. B **47**, 558 (1993), URL <http://link.aps.org/doi/10.1103/PhysRevB.47.558>.
  - <sup>15</sup> G. Kresse and D. Joubert, Phys. Rev. B **59**, 1758 (1999), URL <http://link.aps.org/doi/10.1103/PhysRevB.59.1758>.
  - <sup>16</sup> J. P. Perdew, K. Burke, and M. Ernzerhof, Phys. Rev. Lett. **77**, 3865 (1996), URL <http://link.aps.org/doi/10.1103/PhysRevLett.77.3865>.
  - <sup>17</sup> C. C. Price and N. B. Perkins, Phys. Rev. Lett. **109**, 187201 (2012), URL <http://link.aps.org/doi/10.1103/PhysRevLett.109.187201>.
  - <sup>18</sup> Y. Yu, L. Liang, Q. Niu, and S. Qin, Physical Review B **87** (2013).
  - <sup>19</sup> The Néel-AFM phase is not considered here because it is never the ground state in our calculation.